Engineering aspects of microwave axion generation and detection experiments using RF cavities

Fritz Caspers

CERN, CH-1211, Genve 23, Switzerland

DOI: http://dx.doi.org/10.3204/DESY-PROC-2010-03/caspers_fritz

Using microwave cavities one can build a resonant microwave-shining-throughwalls experiment to search for hidden sector photons and axion-like particles, predicted in many extensions of the standard model. This talk presents a feasibility study of the sensitivities which can be reached using state of the art technology.

1 Motivation and Introduction

Axions, axion-like particles (ALPs), hidden photons and similar weakly interacting slim particles (WISPs) often occur in models beyond the standard model and may be dark matter candidates. Laser-light-shining-through-the-wall (LSW) experiments like ALPS at DESY are currently the most sensitive probes of WISPs. ALPS exploits a resonant optical cavity in order to enhance the power available for photon – WISP conversion.

The idea is to exploit microwave cavities instead of optical resonators [1, 2, 3]. With current technology increased sensitivity in certain mass range can be expected. The first test experiments have already been done (Livermore; Perth), or are being set-up (Daresbury; Yale).

2 Two Cavity setup with very high isolation

A crucial ingredient for a LSW (Laser-light-shining-through-the-wall) experiment is to achieve sufficient shielding. For the intended sensitivity one has to achieve a shielding of roughly 300 dB (a factor 10^{30} in power) between the emitter and the receiver cavity.

Both, the emitting and receiving cavity will be shielded. For the transmitter leakage a good reference level is the ambient electromagnetic parasitics level (cell phones, radio and TV stations etc.) which is usually many orders of magnitude above the thermal noise level. As we cannot keep this background noise below a certain level, the more critical shielding part will be on the receiver side.

One can obtain and measure realistically and in a straightforward manner a shielding value of about 100 dB in a single shell (box) by conventional means in the RF and microwave range (of course higher values are possible). These kind of shielding shells are usually demountable and not soldered. Many examples for this can be found in stochastic cooling systems but also all kind of modern microwave electronics and RF systems in particle accelerators.

The receiving side demands higher requirements and the box-in-the-box concept can be applied, summing up the attenuation of the individual shielding shells in logarithmic scale (i.e.

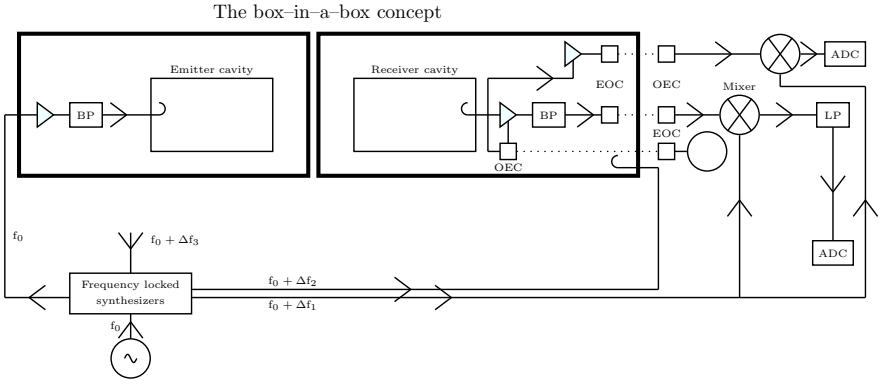

Figure 1: The box-in-a-box concept [3].

multiplying in linear scale) [3]. The innermost shielding layer is provided by the receiving cavity itself.

However, in order to provide sound test data, the shielding between those boxes needs to be constantly monitored and recorded over the full lifetime of the experiment. This makes sure that one is not fooled by electromagnetic leakage (the shielding might degrade due to bad and ageing contacts).

Test tones with the frequency f_0 are emitted between the particular shielding shells [3]. They are small signals in the μW range on different frequencies ($f_0 + \Delta f_2$, $f_0 + \Delta f_3$). Inside the first shell of the receiving setup, the signals are detected by a pick up antenna (PU). The amplitude of the test tone $f_0 + \Delta f_3$ allows the quantification of any potential leakage through the outermost shielding layer. This PU antenna will also see – if there is leakage from the transmitting cavity – signals at f_0 (which would be a veto condition for the measurement). The same principle is used to monitor the second shell with the signal $f_0 + \Delta f_2$ emitted in the first shielding box and detected inside the receiving cavity. By looking for the test signals in our signal spectrum we can evaluate the leaked signals and determine the amount of shielding achieved (of course in the desirable case where we observe no signal at this frequency we know the minimal amount of shielding).

The detected signals are then fed into a mixer where it is combined, i.e., multiplied with the local oscillator on $f_0 + \Delta f_1$ (superheterodyne concept). It is about 20 to 30 kHz offset from the carrier f_0 since the desired intermediate frequency is in the audio range (otherwise we could get too much data for a 2 weeks signal observation and to avoid frequencies from DC to a few kHz in order to eliminate 1/f noise). It then passes through a low frequency band pass filter, is converted into a digital data with an analog digital converter (ADC) and is then recorded. The last bandpass filter reduces the total amount of noise by eliminating the noise from high frequencies where we do not expect a signal. The recorded signal will then be analyzed with a FFT method. A proper signal should appear at frequency Δf_1 in the Fourier analysis.

We have to transport signals and small amounts of DC power for preamplifiers and signal converters through those shells (receiver side) without degrading the performance of the shield-

ing. The number of cables going in and out of the cavity needs to be minimized. It is likely that the only reliable way to do this is using optical transmission for RF/microwave signals, but also of getting in a (needs clarifying) few Watt of DC power for feeding the small signal amplifiers and mixers. We then use an electro optical converter (EOC) to change the signal into an optical signal which is then transmitted to the outside of the box by a glass fibre (dotted lines) where it is reconverted with an opto-electrical converter (OEC). In a similar way the power to the amplifier is fed in with an EOC-OEC set.

2.1 Optical Link on Receiver side

Such DC power transmission using optical fibers (with LEDs at one end and photocells on the other side) was been developed about 30 years ago to supply DC power to small electronic units on high voltage potential in HV transmission systems. Commercial systems for optical fiber based DC power transmission (5 Watt) are available from industry [7], but there is a question mark about how well they would work at cryo-temperatures and / or in very strong magnetic fields.

3 A mHz range observation bandwidth setup

One advantage of the microwave-shining-through-walls setup is that the frequency of the detected signal is exactly at the same frequency as used to produce the new particles. This can be used to suppress noise – and therefore improve signal to noise – by using a narrowband detection method.

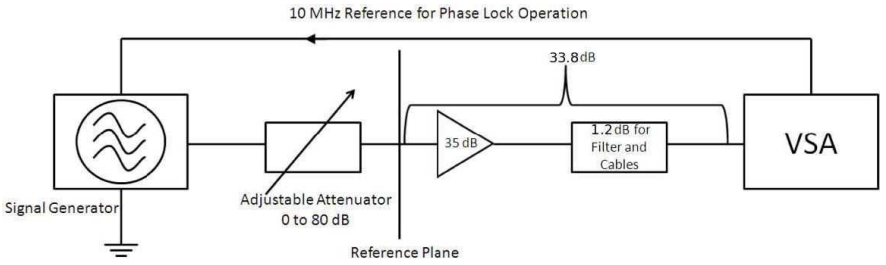

Figure 2: Measurment scheme [4]

A simple test experiment has been performed with standard RF instrumentation in order to crosscheck feasibility of very low observation bandwidth implementation [4]. Using a commercially available vector spectrum analyzer (Agilent 9020 MXA) and a standard low-noise amplifier a sensitivity for a detection of $10^{-22}W$ with 10 measurements of 300 s each has been demonstrated at room temperature [4]. A weak signal is generated in the signal generator and is then further attenuated down to -190 dBm = $10^{-22}W$. This signal is then amplified by a total of 33.8 dB and combined (i.e. mixed) with the reference signal in the vector spectrum analyzer which also records the signal and performs the FFT. In the lower panel the observed signal averaged over 10 measurements (this smoothes out the fluctuations of the envelope of the narrowband filtered and peak detected noise) is shown (the resolution bandwidth is 3 mHz).

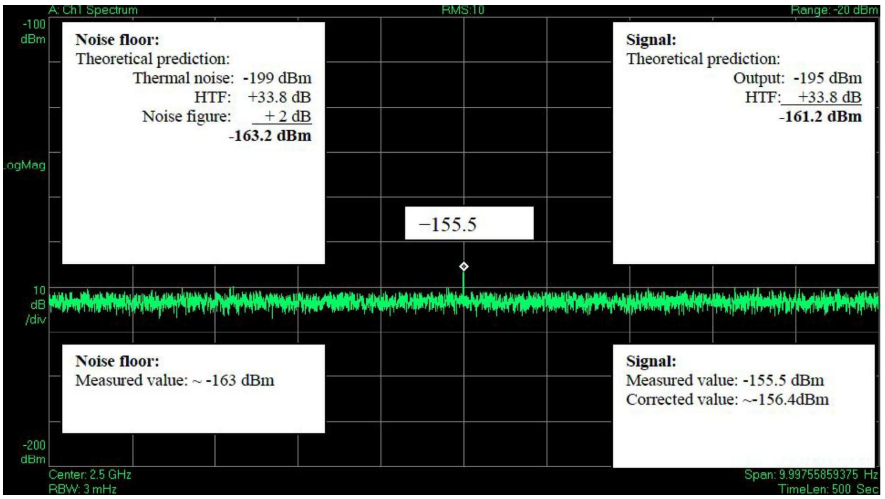

Figure 3: Measured results [4]

A narrow signal line is observed which is clearly distinct from thermal background (-199 dBm) plus the noise from the amplifier (2dB).

In a more advanced setup at cryogenic temperatures we can assume noise temperatures of the order of 10 K. Combining this with integration times of the order of 1000 s we theoretically achieve a sensitivity of $1.4 \cdot 10^{-25} W$. At a frequency of 5 GHz this corresponds to a tiny flux of 0.04 photons per second [3].

Thus by reducing the observation bandwidth down to the mHz or μHz range, we can gain a lot on thermal noise background reduction, provided that the frequency of our converted axions is defined with the same resolution.(i.e. RF cavity generation and receiver concept).

4 Rectangular waveguide TE_{10n} resonator in a LHC magnet

So far, much of the discussion over the last years on axion emitter and receiver cavities has been focused on single mode type cavities (e.g. TM_{010} mode in a pillbox and a solenoid magnet around). Essentially we are aiming for a situation where the RF electric field is parallel to the DC magnetic field over a volume as large as possible. When going to higher frequencies with single mode cavities the volume is getting inevitably smaller and thus also the receiver cross-section and sensitivity for a given distance between emitter and receiver cavity. For a single mode cavity we cannot expect a very strong directionality in the antenna diagram since the maximum linear dimension of the radiating volume (and accordingly by reciprocity for the receiver antenna) is comparable to a single free space wavelength. Higher order mode (with a well defined mode pattern) radiating and receiving structures should exhibit an axion radiation pattern with much better antenna directivity as compared to an elementary dipole. This raises the idea to use the a TE_{101} mode waveguide in the bore of an LHC Magnet.

For the waveguide in the LHC magnet, z would be along the beam axis and y in the direction

of the static magnetic field (up to 8 Tesla).

The Q values of different types of waveguide and coaxial line resonators as a function of frequency are given in [5]. For the TE_{101} resonator (rectangular waveguide with aspect ratio 2/1) we can assume an unloaded Q value of about 8000 for 10 GHz (X-band) at room temperature and no magnetic field. At cryogenic temperatures assuming copper with a RRR value of 100 the Q would be 10 times higher, but due to the magneto-resistance in the end probably just better by a factor of 3.5.

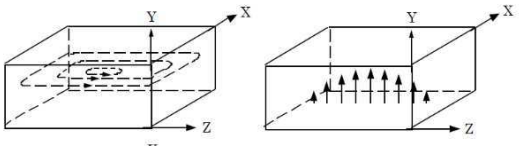

Figure 4: TE_{101} mode pattern in a rectangular waveguide.

Rectangular waveguide dimensions from L-band up to X-band (8.2 to 12.4 GHz) can be found in [5]. The CW power handling capability of an X-band waveguide in air is roughly 200 kW. A X-band waveguide would nicely fit into the beam-screen of an LHC magnet. For higher frequencies i.e. around 100 GHz one may consider a package of say up 20 waveguide in parallel.

The losses for (non overmoded) metallic waveguides increase dramatically towards higher frequencies and accordingly the power handling capability decreases. One can gain about a factor of 10 in losses by using overmoded waveguides (tallguide). As an alternative, above 50 GHz dielectric waveguides with a metallic shielding become interesting since they have much lower losses compared to conventional metallic structures of the same size.

We may consider using an anti-cryostat for the axion transmitter part, thus we would no longer be restricted by the cryo power dissipation limit of 2 Watt per meter of the LHC main dipole beam screen. We could also apply water cooling along the 15 meter long waveguide and possibly dissipate a CW power of 10 kW maybe even 100 kW. Of course this does not make sense for the receiver cavity since low-noise temperature is required. An anti-cryostat has been designed and successfully tested inside a LHC dipole magnet for the purpose of performing magnetic measurements [6]. Its internal temperature was 300 K.

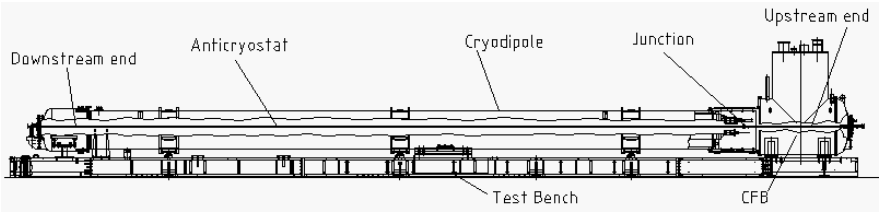

Figure 5: Anti-cryostat.

Another important point is the medium inside the waveguide on the (warm) transmitter side. Air can be better than vacuum as multipacting has to be considered. A quick analysis with the ESA (European Space Agency) multipactor calculator [8] shows that in vacuum and without magnetic field we are all ready for 10 kW power from the generator in a critical region. (But those results need to be re-checked with a magnetic field present)

5 Axion radiation patterns

The waveguide inside the LHC magnet can serve as a phased array antenna. These kind of slotted atennas are widely used e.g. in maritime radars but also for final approach landing radar on airports and of course for all kind of military applications. There is a strong analogy to the axion radiation (and reception) pattern. The slots allow the concentration of the electromagnetic radiation towards the receiving cavity. They are not centered, in order to cut through wall currents and thus provide an electric and magnetic polarization of each slot. This kind of antenna structure (often at higher frequencies than shown here) can be used in standing and in travelling wave mode.

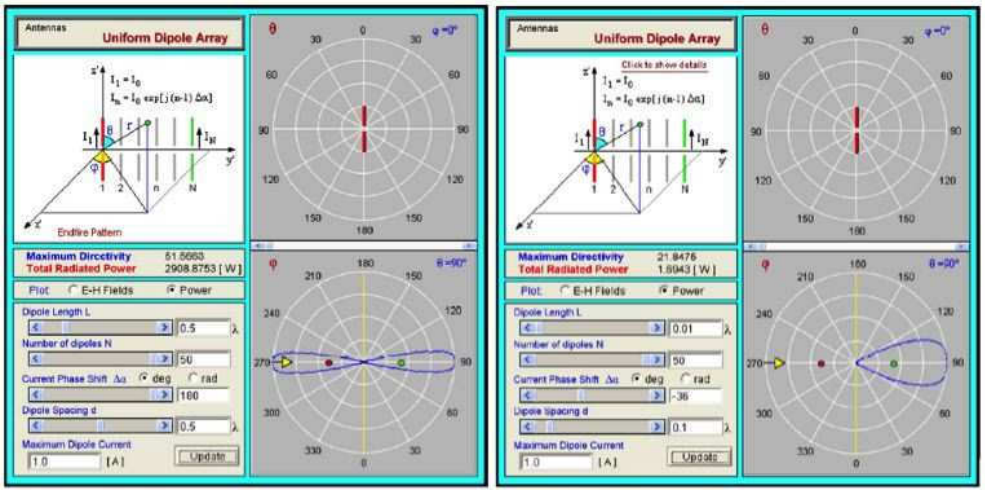

Figure 6: Axion antenna diagrams.

Both is shown in Figure 6. On the left we see nicely the forward and backward radiation lobe ($\phi = 90$ and 270 degree respectively). This case corresponds to the standing wave pattern of a laser beam or coaxial line without dielectric material. As a reminder, the basic law of antenna design: The radiation characteristic of a group of radiating elements in this example is equal to the characteristic of the group (isotropic radiators) to be multiplied with the characteristic of the individual radiator (e.g. dipole). The directional diagram of an empty coaxial line is the same as the Fabry Perot resonator like it is used for axion search in CAST. Thus one might consider using the other bore of the CAST magnet for such a TEM line with about 40 mm outer diameter and operate it in the travelling wave or standing wave mode. A sensitive microwave radiometer used as broadband detector in the range of 2 to 4 GHz bandwidth could detect microwave noise temperature differences in the order of a few μK depending on the orientation of the sun, or any other potential celestial axion source, to the CAST magnet.

On the right side we have the radiation pattern of a travelling wave antenna (end-fire antenna). Note that the relative spacing of the radiating elements is smaller than in the last slide i.e. the antenna is shorter and thus the directional diagram becomes wider. This case corresponds to the travelling wave pattern of a laser beam (v=c).

6 Conclusion and Outlook

In this note we have argued that microwave cavity experiments can provide a powerful tool to search for weakly interacting sub-eV particles, in particular for hidden sector photons and axion-like particles.

The electromagnetic interference problem, in particular for the receiver cavity is an important issue for microwave axion detection experiments. Here the combination of the box-in-the-box concept, together with optical fiber powered diagnostic equipment in the space between the first shielding and the actual cavity, can make a significant contribution. Very narrow band signal detection using, for example 10 days trace record with about 50 Giga samples and 24 bit vertical resolution. This should return via FFT a μHz resolution and related thermal noise reduction. A phaselock method capable of reducing the relative phase noise down the μHz level has been presented and discussed. Higher order mode emitter and receiver cavities, possibly in one or in two LHC magnets were discussed and analyzed in terms of their axion radiation pattern (far field). Highly directional axion emitter and receiver structures may significantly increase the probability of detection.

Acknowledgements

The author would like to thank the CERN AB department management (P. Collier) and in particular the AB-RF group (E. Ciapala) for support as well as Steve Myers and R. Heuer for encouragement. Many thanks to A. Ringwald and J. Jäckel for a large number of hints and inspiring discussions and K. Zioutas for having brought the right people in the right moment together as well as having given very helpful comments.

References

[1] F. Hoogeveen, “Terrestrial axion production and detection using RF cavities”, Physics Letters B, Volume 288, Issues 1-2 (1992).

[2] J. Jaeckel, A. Ringwald, “A Cavity Experiment to Search for Hidden Sector Photons”, Physics Letters B 659:509-514 (2008)

[3] F. Caspers, J. Jaeckel, A. Ringwald, “Feasibility, engineering aspects and physics reach of microwave cavity experiments searching for hidden photons and axions”, IOP Publishing for SISSA (2009).

[4] Caspers et al., “Demonstration of 10-22 Watt signal detection methods in the microwave range at ambient temperatures”, CERN BE-Note 2009-026 (2009).

[5] T. Saad, “Microwave engineers handbook”.

[6] O. Dunkel, P. Legrand and P. Sievers, “A warm bore anticryostat for series magnetic measurements of LHC superconducting dipole and short straight section magnets”, LHC Project Report 685 (2003).

[7] Photonic Power Module PPM-5 from JDSU Company, `http://www.jdsu.com` (2010).

[8] Multipactor Calculator from ESA, `http://multipactor.esa.int/index.html` (2010).

CAST: Recent Results & Future Outlook

T. Papaevangelou[1], *S. Aune*[1], *K. Barth*[2], *A. Belov*[3], *S. Borghi*[2,*], *H. Bräuninger*[4], *G. Cantatore*[5], *J. M. Carmona*[6], *S. A. Cetin*[7], *J. I. Collar*[8], *T. Dafni*[6], *M. Davenport*[2], *C. Eleftheriadis*[9], *N. Elias*[2], *C. Ezer*[7], *G. Fanourakis*[10], *E. Ferrer-Ribas*[1], *H. Fischer*[11], *J. Franz*[11], *P. Friedrich*[4], *J. Galán*[6], *A. Gardikiotis*[12], *E. N. Gazis*[13], *T. Geralis*[10], *I. Giomataris*[1], *S. Gninenko*[3], *H. Gómez*[6], *E. Gruber*[11], *T. Guthörl*[11], *R. Hartmann*[14,†], *F. Haug*[2], *M. Hasinoff*[15], *D. H. H. Hoffmann*[16], *F. J. Iguaz*[6,24], *I. G. Irastorza*[6], *J. Jacoby*[17], *K. Jakovčić*[18], *D. Kang*[11,‡], *T. Karageorgopoulou*[13], *M. Karuza*[5], *K. Königsmann*[11], *R. Kotthaus*[19], *M. Krčmar*[18], *K. Kousouris*[10], *M. Kuster*[4,16,§], *B. Lakić*[18], *P. Lang*[16], *C. Lasseur*[2], *J. M. Laurent*[2], *A. Liolios*[9], *A. Ljubičić*[18], *V. Lozza*[5], *G. Lutz*[14,23], *G. Luzón*[6], *D. W. Miller*[8,¶], *A. Mirizzi*[19,‖], *J. Morales*[6,**], *T. Niinikoski*[2], *A. Nordt*[4,16,], *M. J. Pivovaroff*[20], *G. Raiteri*[5], *G. Raffelt*[19], *T. Rashba*[21], *H. Riege*[16], *A. Rodríguez*[6], *M. Rosu*[16], *J. Ruz*[6,2], *I. Savvidis*[9], *Y. Semertzidis*[12,††], *P. Serpico*[2], *P. S. Silva*[2], *S. K. Solanki*[21], *R. Soufli*[20], *L. Stewart*[2], *A. Tomás*[6], *M. Tsagri*[12,2], *K. van Bibber*[20], *T. Vafeiadis*[2,9], *J. Villar*[6], *J. K. Vogel*[11,20], *L. Walckiers*[2], *Y. Wong*[2], *S. C. Yildiz*[7], *K. Zioutas*[2,12]

1. IRFU, Centre d'Études Nucléaires de Saclay (CEA-Saclay), Gif-sur-Yvette, France
2. European Organization for Nuclear Research (CERN), Genève, Switzerland
3. Institute for Nuclear Research (INR), Russian Academy of Sciences, Moscow, Russia
4. Max-Planck-Institut für extraterrestrische Physik, Garching, Germany
5. Instituto Nazionale di Fisica Nucleare (INFN), Sezione di Trieste and Università di Trieste, Trieste, Italy
6. Instituto de Física Nuclear y Altas Energías, Universidad de Zaragoza, Zaragoza, Spain
7. Dogus University, Istanbul, Turkey
8. Enrico Fermi Institute and KICP, University of Chicago, Chicago, IL, USA
9. Aristotle University of Thessaloniki, Thessaloniki, Greece
10. National Center for Scientific Research "Demokritos", Athens, Greece
11. Albert-Ludwigs-Universität Freiburg, Freiburg, Germany
12. Physics Department, University of Patras, Patras, Greece
13. National Technical University of Athens, Athens, Greece
14. MPI Halbleiterlabor, München, Germany
15. Department of Physics and Astronomy, University of British Columbia, Vancouver, Canada
16. Technische Universität Darmstadt, IKP, Darmstadt, Germany
17. Johann Wolfgang Goethe-Universität, Institut für Angewandte Physik, Frankfurt am Main, Germany
18. Rudjer Bošković Institute, Zagreb, Croatia

[*] Present address: Department of Physics and Astronomy, University of Glasgow, Glasgow, UK
[†] Present address: PNSensor GmbH, München, Germany
[‡] Present address: Karlsruher Institut für Technologie (KIT), Karlsruhe, Germany
[§] Present address: European XFEL GmbH, Notkestrasse 85, 22607 Hamburg, Germany
[¶] Present address: Stanford University and SLAC National Accelerator Laboratory, Stanford, CA, USA
[‖] Present address: Institut für Theoretische Physik,Universität Hamburg, Hamburg, Germany
[**] Deceased
[††] Present address: Brookhaven National Laboratory, New York, USA